LOW-COMPLEXITY NEAR-ML DETECTION ALGORITHMS FOR *N*R-STAR-*M*QAM SPATIAL MODULATION

R. Pillay[1], H. Xu[2] and N. Pillay[3]

School of Engineering, Department of Electrical, Electronic and Computer Engineering, King George V Avenue, Durban 4041, University of KwaZulu-Natal, South Africa.
E-mail: [1]208514668@stu.ukzn.ac.za, [2]xuh@ukzn.ac.za, [3]pillayn@ukzn.ac.za

Abstract: In this study, the authors propose two low-complexity near-maximum-likelihood (ML) detection algorithms for spatial modulation (SM) systems, employing the new multiple-ring star-*M*-ary quadrature amplitude modulation (*N*R-STAR-*M*QAM) constellation. The proposed detectors exploit the specific orientation of *N*R-STAR-*M*QAM, in order to avoid searching across all constellation points. As a result, the computational complexity is independent of both the constellation size and the number of rings presented in *N*R-STAR-*M*QAM. In addition, these detectors are generalized and can be applied to the entire star-*M*QAM family. The Monte Carlo simulation results demonstrate that the proposed detection algorithms achieve the same average bit error rate (ABER) as ML detection for SM but at a much lower computational complexity. For example, in a 4×4, 2R-STAR-16QAM aided SM system, the proposed optimal and sub-optimal detectors achieve an 88.8% and 90.5% reduction in computational complexity, respectively, compared to the ML detector. Furthermore, the simulation results are supported by a closed-form union-bound theoretical ABER expression.

Keywords: Low-complexity near-maximum-likelihood detection, multiple-input multiple-output, *N*-rings star-*M*-ary quadrature amplitude modulation, spatial modulation.

1. INTRODUCTION

Spatial modulation (SM) is a relatively new transmission scheme developed to reduce the cost and complexity of conventional multiple-input multiple-output systems [1]. In SM, only one transmit-antenna is active during each transmission interval, which effectively means that inter-channel interference (ICI) is completely avoided and inter-antenna synchronization (IAS) is not needed [2]. The transmission of information in SM can be described as a simple approach; the transmitter uses the index of the activate antenna, which is determined by the bitstream to be transmitted, as an additional means to convey information in conjunction with the use of conventional amplitude/phase modulation (APM) constellation, i.e., *M*-ary phase shift keying (*M*PSK) or *M*-ary quadrature amplitude modulation (*M*QAM) [3].

At the receiver, the need to correctly detect the transmitted information bitstream is of utmost importance. In [3], Jeganathan *et al.* derived an optimal detection algorithm for SM based on the maximum-likelihood (ML) method. This detector involves the joint estimation of the transmit-antenna index and the transmitted symbol. Although optimal error performance is achieved, the detector imposes a very high search complexity that grows as $N_T M$, where N_T and M represent the number of transmit antennas and the modulation order of the employed APM constellation, respectively. This high receiver complexity poses a considerable challenge for practical implementation. In order to address this problem, several researchers have proposed low-complexity detection algorithms for SM [4]-[12]. In [4], the authors proposed a multistage (MS) detection algorithm that operates over two steps. The first step selects the most probable estimates of the active transmit-antenna index based on the modified maximum ratio combiner (MMRC) method. The second step uses the ML method to detect the transmitted symbol. However, the MS detector imposes a high computational complexity for large order APM constellations. In [5], a simple detection algorithm for *M*QAM aided SM (*M*QAM-SM) systems was developed. This algorithm was based on searching partitioned symbol sets for the active transmit-antenna index and transmitted symbol. Then in [6], a distance-based ordered detection (DBD) algorithm was proposed and was aimed at achieving a flexible trade-off between error performance and computational complexity. In [7], the authors proposed two-sphere decoding algorithms that were tailored for specific SM systems. It was shown that the computational complexity of these algorithms grows linearly with the constellation size. In [8], Rajashekar *et al.* proposed a hard-limiter based ML detector whose computational complexity is independent of M and only grows with N_T. However, this detector is specific for SM systems employing the rectangular-*M*QAM and square-*M*QAM constellations. In [9]-[10], a signal vector-based detection (SVD) algorithm was presented. Although the receiver complexity of SVD is very much lower than that of ML, it demonstrated some performance loss in *M*QAM-SM systems. Meanwhile in [11], the authors proposed a novel detection algorithm specific for *M*PSK aided SM systems. This detector was shown to achieve the same error performance of ML detection but at a complexity that is independent of M. Recently, the authors of [12] proposed two innovative low-complexity detectors for SM employing the *M*-ary

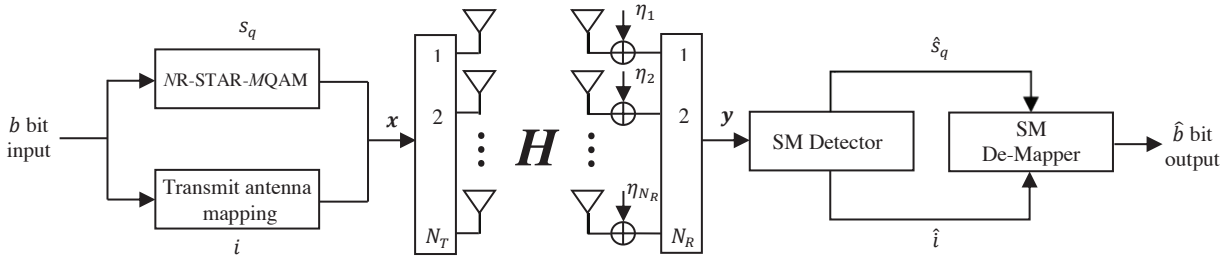

Figure 1: System model of NR-STAR-MQAM aided SM [4].

amplitude-PSK (M-APSK) constellation. The M-APSK constellation belongs to the family of star-MQAM constellations, namely: conventional star-MQAM [13], M-APSK [14] and new dual-ring star-MQAM [15]. This family outperforms the conventional APM constellations in terms of achievable mutual information over peak-power-limited systems [15]-[16]. Hence, it has been widely adopted in most satellite and space communication standards, such as 2nd generation digital video broadcasting system (DVB-S2), internet protocol over satellite (IPoS) and advanced broadcasting systems via satellite (ABS-S) [13]-[16]. Consequently, the motivation and contributions of this paper are:

1.1. Motivation

Based on the above background, SM provides many attractive advantages for next generation networks. It is useful to note that single-symbol and multiple-symbol generalised SM (GSM) [17]-[21] address the constraint on the number of required transmit antennas in SM to achieve high spectral efficiency. It was shown in [17] that single-symbol GSM has an inferior error performance compared to SM, while the drawback of multiple-symbol GSM [18]-[21] is the very high hardware complexity due to multiple radio-frequency chains, ICI and the need for IAS. Hence, this motivates us to investigate SM.

Although the low-complexity detectors of [12] achieve near-ML error performance, these detectors are specific to SM systems employing only the M-APSK constellation. Furthermore, the computational complexities of these detectors have been shown to be independent of M but linearly dependent on both N_T and the number of rings (N) presented in the M-APSK constellation. Moreover, these detectors require pre-processing at the receiver, which can easily translate into additional hardware costs.

Despite the merits of the M-APSK constellation [12], [14], the rest of the star-MQAM family may prove beneficial for different systems. For instance, in SM systems, the new dual-ring star-16QAM slightly outperforms the popular square-16QAM in terms of error performance [15]. Based on this research, we have extended the new dual-ring star-MQAM to multiple-ring star-MQAM [22], which is denoted as NR-STAR-MQAM for simplicity. It was shown in [22] that NR-STAR-MQAM utilizes up to 98% less average signal energy, and has fewer amplitude levels and phase differences than its square-MQAM counterpart. In addition, this constellation is superior to other multiple-ring constellations [23]-[24], in terms of improving error performance and deriving a closed-form solution.

1.2. Contributions

Based on the above motivation, the contributions of this paper are: we propose two low-complexity near-ML detection algorithms for SM systems employing any constellation from the star-MQAM family [12]-[15], which is now inclusive of NR-STAR-MQAM [22]. Unlike the detectors in [12], which are specific to M-APSK aided SM (M-APSK-SM) systems, the proposed detectors are generalized and can be applied to SM employing any multiple-ring constellation. Based on the work in [11]-[12], we achieve the proposed detection algorithms by exploiting the key features of the star-MQAM family. Due to the advantages of NR-STAR-MQAM [22], we investigate the average bit error rate (ABER) of the proposed detectors in SM systems employing said constellation. Furthermore, we show that the computational complexities of the proposed detection algorithms are independent of both the constellation size and the number of rings presented in the NR-STAR-MQAM constellation.

Organization: Section 2 details the NR-STAR-MQAM aided SM (NR-STAR-MQAM-SM) system model and the features of the star-MQAM family. Section 3 presents the proposed low-complexity near-ML detection algorithms. In Section 4, the computational complexities of the proposed detection algorithms are formulated. Section 5 demonstrates and discusses the numerical results of the work. Finally, concluding remarks are drawn in Section 6.

Notation: Bold lowercase and uppercase letters are used for column vectors and matrices, respectively. $[\cdot]^T$, $|\cdot|$ and $\|\cdot\|_F$ represents the transpose, Euclidean norm and Frobenius norm, respectively. $\underset{w}{\text{argmin}}(\cdot)$ and $\underset{w}{\text{argmax}}(\cdot)$ operators represent the minimum and maximum of the argument with respect to w, respectively. $\text{argmax}_w^{\bar{N}}(\cdot)$ operator selects the $\bar{N}$ values of w which maximize the argument. $E\{\cdot\}$ is the mathematical expectation and $(\cdot)^*$ represents the conjugate of the vector. $\Re(\cdot)$ and $\Im(\cdot)$ represent the real and imaginary part of the complex

argument, respectively. $\{\cdot\}_{\text{lowerbound}}^{\text{upperbound}}$ represents all possible values of the argument limited to the upper- and lower bounds, and j denotes a complex unit. $\min(\cdot)$ returns the smallest element in an array. $\text{mod}(\text{a}, \text{n})$ denotes that a is the computed modulus of n, $\text{round}(\text{a})$ rounds the element a to its nearest integer and $\lceil \text{a} \rceil$ rounds the element a to the nearest integer greater than or equal to a.

2. *N*R-STAR-*M*QAM-SM SYSTEM MODEL

2.1. SM Transmission and ML Detection

Consider an $N_T \times N_R$, *N*R-STAR-*M*QAM-SM system model shown in Figure 1, where N_T and N_R represent the number of transmit and receive antennas, respectively. The SM mapper assigns a $b = \log_2(MN_T)$ bit binary input to both a transmit-antenna index i $(1 \leq i \leq N_T)$ and a complex-valued transmit symbol s_q $(1 \leq q \leq M)$ from the APM symbol set $\boldsymbol{s}$. Throughout this paper, we consider $\boldsymbol{s}$ to be the *N*R-STAR-*M*QAM constellation [22], unless otherwise stated.

The assignment of i and s_q are defined by the SM mapping table, which is known at both the transmitter and receiver [3]-[5]. The SM mapper output can be expressed as:

$$\boldsymbol{x} = \underset{\substack{1^{st}\text{ position} \\ \downarrow}}{[0} \; 0 \; \ldots \; \underset{\substack{i^{th}\text{ position} \\ \uparrow}}{s_q} \; \ldots \; \underset{\substack{N_T{}^{th}\text{ position} \\ \downarrow}}{0]^T} \tag{1}$$

where $\boldsymbol{x}$ is the $N_T \times 1$ transmit vector, s_q denotes the q^{th} symbol from the *N*R-STAR-*M*QAM constellation with $E\left\{\left|s_q\right|^2\right\} = 1$ and $s_q \in \boldsymbol{s}, \boldsymbol{s} = \{s_1, s_2, \ldots, s_M\}$.

The transmit vector defined by (1) has $N_T - 1$ zero entries corresponding to the dormant transmit antennas and a single non-zero entry s_q at the i^{th} position corresponding to the active transmit-antenna. After the mapping process is completed, the transmit vector $\boldsymbol{x}$ is transmitted over a Rayleigh, frequency-flat fading channel experiencing N_R-dimensional additive white Gaussian noise $\boldsymbol{\eta} = [\eta_1, \eta_2, \ldots, \eta_{N_R}]^T$. The $N_R \times N_T$ channel gain matrix $\boldsymbol{H}$ is given by $\boldsymbol{H} = [\boldsymbol{h}_1 \; \boldsymbol{h}_2 \; \ldots \; \boldsymbol{h}_{N_T}]$, where $\boldsymbol{h}_i$ represents a column vector that is defined as $\boldsymbol{h}_i = [h_{1i} \; h_{2i} \; \ldots \; h_{N_R i}]^T$. The elements of both $\boldsymbol{H}$ and $\boldsymbol{\eta}$ are assumed to be independent and uniformly distributed complex Gaussian random variables with zero mean and unit variance.

The corresponding $N_R \times 1$ received signal vector $\boldsymbol{y}$ is given by:

$$\boldsymbol{y} = \sqrt{\rho}\boldsymbol{H}\boldsymbol{x} + \boldsymbol{\eta} \tag{2}$$

where ρ is the average signal-to-noise ratio (SNR) per receive antenna and the transmit vector $\boldsymbol{x}$ is of the form, $\boldsymbol{x} = s_q \boldsymbol{e}_i$, where the vector $\boldsymbol{e}_i$ is selected from the N_T-dimensional standard basis vectors, e.g., $\boldsymbol{e}_1 = [1, 0, \ldots, 0]^T$ [4]. The set of all $\boldsymbol{x}$ is contained in $\boldsymbol{\Gamma}$.

At the receiver, the SM detector obtains estimates of the transmit-antenna index and transmitted symbol using the ML detection rule, which is given by:

$$(\hat{\imath}, \hat{s}_q) = \underset{\boldsymbol{x} \in \boldsymbol{\Gamma}}{\text{argmin}} \left\| \boldsymbol{y} - \sqrt{\rho}\boldsymbol{H}\boldsymbol{x} \right\|_F^2 \tag{3}$$

where $\hat{\imath}$ and $\hat{s}_q$ represents the estimates of the transmit-antenna index and transmitted symbol, respectively.

In order to gain a better understanding of the proposed detectors, we first introduce the features of the star-*M*QAM family and then briefly explain the latest low-complexity detectors [12].

2.2. Star-MQAM Family of Constellations

The star-*M*QAM family is composed of *N* concentric rings of PSK. In addition, the phase differences between adjacent symbols on the same ring are equal [12]-[15], [22]. The set of constellation symbols $\boldsymbol{s}$ are given as follows:

$$\boldsymbol{s} = \begin{cases} r_1 \exp\left(j\left(\frac{2\pi}{n_1}k + \theta_1\right)\right), k = 0;\ 1; \ldots; n_1 - 1 \\ r_2 \exp\left(j\left(\frac{2\pi}{n_2}k + \theta_2\right)\right), k = 0; 1; \ldots; n_2 - 1 \\ \vdots \\ r_N \exp\left(j\left(\frac{2\pi}{n_N}k + \theta_N\right)\right), k = 0;\ 1; \ldots; n_N - 1 \end{cases} \tag{4}$$

where n_l such that $\sum_{l=1}^{N} n_l = M$, r_l such that $r_1 < r_2 < \cdots < r_N$ and θ_l represents the number of symbols, the radius and the initial phase shift of the l^{th} ring, respectively.

The configuration to denote the number of symbols on each ring is given by $\boldsymbol{n} = (n_1, n_2, \ldots, n_N)$. In Figure 2, the conventional star-16QAM [13], 16-APSK [14] and the new class of dual-ring star-16QAM [15] constellations are shown, respectively. Note, these dual-ring constellations are the foundation of any multiple-ring constellation that can be both Gray mapped and theoretically validated. The multiple-ring constellations in [23]-[24], do not inherit the features of the dual-ring constellations in Figure 2 and hence, not viable options to both improve and evaluate the ABER performance of SM systems. Nevertheless, the proposed detectors can still be applied to these irregular constellations [23]-[24].

Table 1 presents the different number of amplitude and phase types of the conventional star-16QAM, 16-APSK,

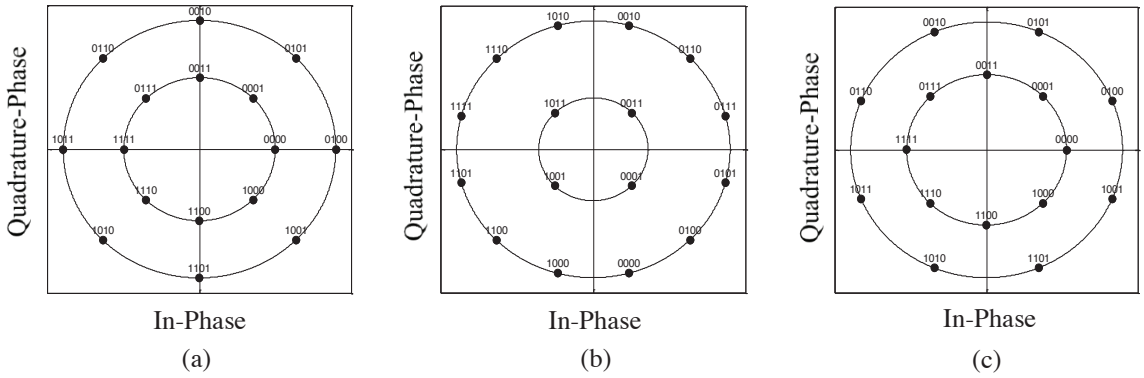

Figure 2: The dual-ring star-*M*QAM family, a) Conventional star-16QAM, $\boldsymbol{n} = (8,8)$, b) 16-APSK, $\boldsymbol{n} = (4,12)$, and c) New dual-ring star-16QAM, $\boldsymbol{n} = (8,8)$.

new dual-ring star-16QAM and the popular square-16QAM constellation [22]-[23]. It can be seen that the star-16QAM family has fewer amplitudes and phase types than the square-16QAM constellation. This indicates that the star-*M*QAM family has a stronger ability to resist errors than its square-*M*QAM counterpart [22]-[23]. For example, square-16QAM has 3 different amplitude and 12 different phase types, whereas conventional star-16QAM has 2 different amplitude and 8 different phase types.

Table 1: Amplitude and Phase Types of the star-16QAM Family and square-16QAM Constellations [22]-[23].

APM Constellation	Amplitude Types	Phase Types
Conventional star-16QAM	2	8
16-APSK	2	12
New dual-ring star-16QAM	2	16
Square-16QAM	3	12

Compared to the multiple-ring constellations in [23]-[24], *N*R-STAR-*M*QAM is superior in terms of matching with Gray mapping, error performance and being able to easily derive a closed-form solution [22]. Hence, we investigate the proposed detectors in *N*R-STAR-*M*QAM-SM systems. The multiple-ring constellations sizes of interest are the 2R-STAR-16QAM, 4R-STAR-64QAM and 8R-STAR-256QAM. These constellations were designed, based on achieving almost the same Euclidean distance as the square-16QAM, square-64QAM and square-256QAM constellations, respectively, by using as few rings as possible [22]-[23].

2.3. Latest Low-Complexity near-ML Detection Algorithms

The authors of [12] developed two low-complexity detection algorithms for SM systems employing the *M*-APSK constellation (Figure 2(b)). The first detection algorithm achieves optimal-ML performance and consists of two steps. The first step lies in identifying the most probable ring in the *M*-APSK constellation to which the receive signal vector belongs to, and is defined as:

$$z_i = \frac{\boldsymbol{h}_i^H \boldsymbol{y}}{\|\boldsymbol{h}_i\|_F^2}, i \in 1; \dots; N_T \tag{5}$$

In order to achieve the desired outcome of the first step, the receiver is required to perform a few preprocessing tasks that create a threshold decision rule. The computational complexity of this rule may grow depending on the number of rings presented in the *M*-APSK constellation. Let $\hat{l}$ be the estimated ring at the end of the first step.

Then, step 2 involves jointly estimating the transmit-antenna index and transmitted symbol. At this point, the search space of the transmitted symbol is reduced from *M* to the number of symbols that lie on the $\hat{l}^{th}$ ring and is given by:

$$\boldsymbol{s}_{\hat{l}} = r_{\hat{l}} \exp\left(j\left(\frac{2\pi}{n_{\hat{l}}}k + \theta_{\hat{l}}\right)\right), k = 0; 1; \dots; n_{\hat{l}} - 1 \tag{6}$$

Once (6) has been determined, the most probable symbol on the $\hat{l}^{th}$ ring can be determined using [12, Eq. (26)]. Then by using [12, Eq. (27)] the estimated transmit-antenna index can be determined.

The second low-complexity detection algorithm in [12] achieves sub-optimal ML performance and also consists of two steps. The first step selects the $\bar{N}$ most probable transmit-antenna indices, based on the MMRC [4]-[5] criterion and is described as:

$$\boldsymbol{w} = \arg\max_{i \in [1:N_T]}^{\bar{N}} (|z_i|) \tag{7}$$

The second step jointly estimates the transmit-antenna index from the $\bar{N}$ candidates and the transmitted symbol using the optimal-ML detection algorithm.

Despite the ingenuity of the above-mentioned algorithms, there are two notable disadvantages. Firstly, these algorithms are only suited for SM systems employing the *M*-APSK constellation. Secondly, the pre-processing tasks at the receiver may add to overall hardware cost of the system.

Hence, to alleviate these disadvantages, we formulate two near-ML low-complexity detection algorithms, which are presented in the next section.

3. PROPOSED DETECTION ALGORITHMS

In this section, we propose two near-ML low-complexity detectors for *N*R-STAR-*M*QAM-SM systems. Unlike the latest low-complexity detectors [12], which are only suited for SM employing the *M*-APSK constellation, the two proposed detectors are generalized and can be applied to SM employing any constellation from the star-*M*QAM family. Note that any multiple-ring constellations, despite both its structure and orientation, belongs to the star-*M*QAM family.

3.1. Proposed Low-Complexity Optimal Near-ML Detection Algorithm

The proposed optimal near-ML detection algorithm for SM systems operates over two steps. The first step involves detecting the two rings closest to (5) and lastly, the second step involves jointly estimating the transmitted symbol and the transmit-antenna index.

Step 1: The first step is aimed at determining the two rings closest to $\boldsymbol{z}_i$. This is achieved using, step 3 to step 7, in Algorithm 1. Note the estimates of the two closest rings are stored in $\boldsymbol{t}$.

Once the two most probable rings have been determined, the search space of the second step has been reduced to the symbols that lie on the estimated two rings and is given by [11]-[12]:

$$\boldsymbol{s_t} = \begin{cases} r_{\boldsymbol{t}(1)} \exp\left(j\boldsymbol{\varphi}_{\boldsymbol{t}(1)}\right) \\ r_{\boldsymbol{t}(2)} \exp\left(j\boldsymbol{\varphi}_{\boldsymbol{t}(2)}\right) \end{cases} \tag{8}$$

where $\boldsymbol{\varphi}_{\boldsymbol{t}(1)}$ and $\boldsymbol{\varphi}_{\boldsymbol{t}(2)} \in \boldsymbol{\varphi_t}$, $\boldsymbol{\varphi_t} = \left\{\frac{2\pi}{n_{\boldsymbol{t}(\bar{w})}} k_{\boldsymbol{t}(\bar{w})} + \theta_{\boldsymbol{t}(\bar{w})}, k_{\boldsymbol{t}(\bar{w})} = 0, 1, \ldots, n_{\boldsymbol{t}(\bar{w})} - 1\right\}_{\bar{w}=1}^{\bar{w}=2}$ and $r_{\boldsymbol{t}(1)}, r_{\boldsymbol{t}(2)} \in \boldsymbol{r_t}$, with $r_{\boldsymbol{t}(1)} < r_{\boldsymbol{t}(2)}$.

Step 2: The ML-based criterion of (3) can be split-up into an inner- and outer optimization problem that can be rewritten as:

$$\left(\hat{\imath}, \hat{s}_q\right) = \underset{i \in [1:N_T]}{\operatorname{argmin}} \left(\min_{s_q \in \boldsymbol{s_t}} \left\| \boldsymbol{y} - \sqrt{\rho}\boldsymbol{h}_i s_q \right\|_F^2 \right) \tag{9}$$

For a given value of i, the inner optimization problem of (9) can be written as $\hat{s}_q = \min_{s_q \in \boldsymbol{s_t}} \left(\left\| \boldsymbol{y} - \sqrt{\rho}\boldsymbol{h}_i s_q \right\|_F^2 \right)$ and is equally described as [11]:

$$\hat{s}_q = \underset{s_q \in \boldsymbol{s_t}}{\operatorname{argmin}} \left(\left| z_i - s_q \right|^2 \right) \tag{10}$$

where $z_i = c_i \exp(j\vartheta_i)$ and $s_q = r\exp(j\varphi)$, respectively.

Then (10) can be further expressed as:

$$\hat{s}_q = \underset{r \in \boldsymbol{r_t}, \varphi \in \boldsymbol{\varphi_t}}{\operatorname{argmin}} \left(|c_i|^2 + |r|^2 - 2c_i r \cos(\vartheta_i - \varphi) \right) \tag{11}$$

The equivalent of (11) can be directly expressed as:

$$\hat{\varphi}_i = \underset{\varphi \in \boldsymbol{\varphi_t}}{\operatorname{argmax}} (\cos(\vartheta_i - \varphi)) \tag{12}$$

The function of (12) is to determine the transmitted symbol $\hat{s}_q$ by comparing the angles of each symbol in $\boldsymbol{s_t}$ to the angle of the receive signal vector z_i. However, this will not work when $\boldsymbol{s_t}$ contains symbols with different amplitude levels. This is because there exists a scenario where a symbol will be chosen based on (12) but another symbol will lie closer to z_i based on Euclidean distance. Note, the latter part of the scenario will obtain the correct result. Hence, we establish a relationship between the orientation of each ring and z_i. Thus for an initial phase shift of $\theta_{\boldsymbol{t}(\bar{w})} = 0$, the relationship can be described as:

$$\hat{\varphi}_{\boldsymbol{t}(\bar{w})} = \mathrm{mod}\left(\mathrm{round}\left(Q_{\hat{\varphi}_{\boldsymbol{t}(\bar{w})}}\right), n_{\boldsymbol{t}(\bar{w})}\right) \times \left(\frac{2\pi}{n_{\boldsymbol{t}(\bar{w})}}\right) \tag{13}$$

where $Q_{\hat{\varphi}_{\boldsymbol{t}(\bar{w})}} = \vartheta_i / \left(2\pi / n_{\boldsymbol{t}(\bar{w})}\right)$ and $\bar{w} = 1, 2$.

In order to accommodate for rings that have an initial phase shift equal to $\theta_{\boldsymbol{t}(\bar{w})} = \left(\pi / n_{\boldsymbol{t}(\bar{w})}\right)$, we formulate a simple expression:

$$\hat{\varphi}_{\boldsymbol{t}(\bar{w})} = \left(\mathrm{mod}\left(\left\lfloor Q_{\hat{\varphi}_{\boldsymbol{t}(\bar{w})}} \right\rfloor, n_{\boldsymbol{t}(\bar{w})}\right) \times \left(\frac{2\pi}{n_{\boldsymbol{t}(\bar{w})}}\right)\right) - \left(\frac{\pi}{n_{\boldsymbol{t}(\bar{w})}}\right) \tag{14}$$

Thus from (13) and/or (14), we can estimate the most probable symbol on each ring as follows [12]:

$$\hat{\boldsymbol{s}}_{\boldsymbol{t}} = \begin{cases} r_{\boldsymbol{t}(1)} \exp\left(j\hat{\varphi}_{\boldsymbol{t}(1)}\right) \\ r_{\boldsymbol{t}(2)} \exp\left(j\hat{\varphi}_{\boldsymbol{t}(2)}\right) \end{cases} \tag{15}$$

By using (10) and (15), we can correctly estimate the transmitted symbol, which is given as:

$$\hat{s}_q = \arg \min_{s \in \hat{\boldsymbol{s}}_{\boldsymbol{t}}} (|\boldsymbol{z}_i - s|^2) \tag{16}$$

After obtaining the correct transmitted symbol $\hat{s}_q$, we estimate the transmit-antenna index by substituting $\hat{s}_q$ in (9), which is given by:

$$\hat{\imath} = \arg\min_{i\in[1:N_T]} \left(\left\| \boldsymbol{y} - \boldsymbol{h}_i \hat{s}_q \right\|_F^2 \right) \quad (17)$$

In order to reduce the complexity of (17), the authors of [8] considered that:

$$\begin{aligned} \left\| \boldsymbol{y} - \boldsymbol{h}_i \hat{s}_q \right\|_F^2 &= \ldots \\ \ldots &= \|\boldsymbol{y}\|_F^2 + \|\boldsymbol{h}_i\|_F^2 \left|\hat{s}_q\right|^2 - 2\Re\left(\boldsymbol{h}_i^H \boldsymbol{y} \hat{s}_q{}^*\right) \\ &= \|\boldsymbol{y}\|_F^2 + \left\{ \left|z_i - \hat{s}_q\right|^2 - |z_i|^2 \right\} \|\boldsymbol{h}_i\|_F^2 \end{aligned} \quad (18)$$

From (17) and (18), we obtain that:

$$\hat{\imath} = \arg\min_{i\in[1:N_T]} \left(\|\boldsymbol{y}\|_F^2 + \left\{ \left|z_i - \hat{s}_q\right|^2 - |z_i|^2 \right\} \|\boldsymbol{h}_i\|_F^2 \right) \quad (19)$$

For the optimization problem of (19), $\|\boldsymbol{h}_i\|_F^2$ does not need to be computed again, which further reduces the computational complexity [8].

Hence the low-complexity optimal near-ML detection algorithm is summarized in Algorithm 1:

Algorithm 1: **Low-complexity optimal-ML detection algorithm for SM employing any multiple-ring constellation**.

1: For $i = 1 : N_T$
2: $z_i = (\boldsymbol{h}_i^H \boldsymbol{y} / \|\boldsymbol{h}_i\|_F^2)$
3: For $l = 1 : N$
4: If $r_l < |z_i| \leq r_{l+1}$
5: $\boldsymbol{t} = l,\ l+1$. Note, when $|z_i| \leq r_1,\ \boldsymbol{t} = 1, 2$ and when $|z_i| > r_N,\ \boldsymbol{t} = N-1, N$.
6: End If
7: End For
8: For $\overline{w} = 1 : \text{length}(\boldsymbol{t})$
9: Obtain $\hat{\boldsymbol{s}}_{\boldsymbol{t}}$ from (15)
10: Compute $\boldsymbol{d}_{\overline{w}}$, where $\boldsymbol{d}_{\overline{w}} = \left(\left| z_i - \hat{\boldsymbol{s}}_{\boldsymbol{t}(\overline{w})} \right|^2 \right)$
11: End for
12: Find the minimum value of $\boldsymbol{d}$ and store index, then $\hat{s}_q(i) = \boldsymbol{d}_{\text{index}}$
13: Compute $\boldsymbol{c}_i = \left\{ \left| \boldsymbol{w}_i - \hat{s}_q(i) \right|^2 - |\boldsymbol{w}_i|^2 \right\} \|\boldsymbol{h}_i\|_F^2$
14: End for
15: Find the minimum value of $\boldsymbol{c}$ and store index*, Output index* and $\hat{s}_q(\text{index}^*)$

3.2. Proposed Low-Complexity Sub-Optimal Near-ML Detection Algorithm

In this subsection, we propose a low-complexity detection algorithm which achieves sub-optimal error performance. This algorithm matches the ABER of SM systems using the MS detection algorithm [4]. However, unlike the MS detection algorithm, the proposed sub-optimal detector is suitable for SM systems that employ large order APM constellations. The proposed low-complexity sub-optimal detection algorithm operates over the following two steps, which are summarized as follows:

Step 1: The first step is aimed at reducing the transmit-antenna search space, which is efficiently achieved by using (7).

Step 2: After reducing the transmit-antenna search space to $\overline{N}$ possible candidates, we then apply Algorithm 1, which is discussed in the previous subsection. Note that z_i does not need to be calculated in Algorithm 2, since the computation of (7) is the same as (5). The sub-optimal ML detection algorithm is summarized in Algorithm 2:

Algorithm 2: **Low-complexity sub-optimal ML detection algorithm for SM employing any multiple-ring constellation.**

1: Determine $\boldsymbol{w}$, using (7)
2: For $i = 1 : \text{length}(\boldsymbol{w})$
3: For $l = 1 : N$
4: If $r_l < \boldsymbol{w}_i \leq r_{l+1}$
5: $\boldsymbol{t} = l,\ l+1$. Note, when $\boldsymbol{w}_i \leq r_1,\ \boldsymbol{t} = 1, 2$ and when $\boldsymbol{w}_i > r_N,\ \boldsymbol{t} = N-1, N$.
6: End If
7: End For
8: For $\overline{w} = 1 : \text{length}(\boldsymbol{t})$
9: Obtain $\hat{\boldsymbol{s}}_{\boldsymbol{t}}$ from (15)
10: Compute $\boldsymbol{d}_{\overline{w}}$, where $\boldsymbol{d}_{\overline{w}} = \left(\left| \boldsymbol{w}_i - \hat{\boldsymbol{s}}_{\boldsymbol{t}(\overline{w})} \right|^2 \right)$
11: End for
12: Find the minimum value of $\boldsymbol{d}$ and store index, then $\hat{s}_q(i) = \boldsymbol{d}_{\text{index}}$
13: Compute $\boldsymbol{c}_i = \left\{ \left| \boldsymbol{w}_i - \hat{s}_q(i) \right|^2 - |\boldsymbol{w}_i|^2 \right\} \|\boldsymbol{h}_i\|_F^2$
14: End for
15: Find the minimum value of $\boldsymbol{c}$ and store index*, Output index* and $\hat{s}_q(\text{index}^*)$

Hence, the proposed sub-optimal ML detection algorithm is a viable option for SM systems that have a large N_T, M or both.

4. COMPUTATIONAL COMPLEXITY ANALYSIS

In this section, we present the computational complexity at the receiver, in terms of the total number of floating point operations (flops) [22] required for both the proposed sub-optimal detector (PSOD) and proposed optimal detector (POD). Thereafter, we compare these detectors to a few other notable SM detectors, i.e., the MMRC detection [4], SVD [9], DBD [6], MS detection [4] and ML-based detection [3]. We assume results required for future

computations can be stored, therefore redundant computation is neglected and full channel knowledge is known at the receiver for all the detection algorithms.

4.1. Formulation of Computational Complexity

ML Detection: It is straightforward from (3) that it can be rewritten as $\left(\hat{\imath}, \hat{s}_q\right) = \arg\min_{i\in[1:N_T]}\left(\min_{s_q\in \boldsymbol{s}}\left(\left\|\boldsymbol{y}-\sqrt{\rho}\boldsymbol{h}_i s_q\right\|_F^2\right)\right)$ and that the order of complexity grows as $N_T M$. For a given $\left(\hat{\imath}, \hat{s}_q\right)$, the complexity imposed by the inner term $\left\|\boldsymbol{y}-\sqrt{\rho}\boldsymbol{h}_i s_q\right\|_F^2 = \sum_{t=1}^{N_R}\left|y_t-\sqrt{\rho}h_{t,i}s_q\right|^2$ is equal to $6N_R$ flops. Hence, the total computational complexity imposed is $\delta_{ML} = 6N_R N_T M$ flops [11]-[12].

Latest low-complexity ML Detection Algorithms: In [12], two detectors, termed PHD and PMML were proposed specifically for *M*-APSK-SM systems. The complexity imposed by both PHD and PMML are $\delta_{PHD} = (6N_R+4)N_T + 9\bar{N} + 4\bar{N}\lceil N/2\rceil$ flops and $\delta_{PMML} = (6N_R+11)N_T + 4N_T\lceil N/2\rceil$ flops, respectively. Note, that the complexity of PHD and PMML matches the complexity of the PSOD and the POD, respectively, only for *M*-APSK-SM systems.

Proposed optimal-ML Detection: It can be seen that Algorithm 1 grows as N_T. The complexity imposed by (5) is $6N_R + 2$ flops [11]-[12]. The computation of calculating the most probable symbol on each ring is equal to a total of 8 flops, according to (15). Then the estimated transmitted symbol is obtained by (16) which amounts to a total of 4 flops. Finally, the computation of (19) which estimates the transmit-antenna index incurs 5 flops, since $\|\boldsymbol{h}_i\|_F^2$ has already been computed while obtaining (5). Hence, the total number of flops imposed is equal to $\delta_{Proposed\ Optimal} = (6N_R+19)N_T$.

Proposed sub-optimal ML Detection: The computation of the first step, which estimates the $\bar{N}$ most probable transmit antenna(s) is equal to $6N_R N_T + 4N_T$ flops [4]. Thereafter, we apply Algorithm 1 but with two slight modifications. Firstly, N_T needs to be replaced by $\bar{N}$. Secondly (5), does not need to be computed because it is the same as (7). Thus the complexity imposed by Algorithm 1 is equal to 12 flops for step 8 to step 11 and 5 flops for estimating the transmit-antenna index. Hence, the total computational complexity imposed is $\delta_{Proposed\ Sub-Optimal} = 6N_R N_T + 4N_T + 17\bar{N}$ flops.

It is worth mentioning that the complexity of Algorithm 1 may be further reduced for SM systems employing the conventional star-*M*QAM constellation (Figure 2(a)). This is because the Euclidean distance between any two neighboring constellation points on adjacent rings are equal. This means that step 3 to step 7 in Algorithm 1 can be easily modified to find the single closest ring to (5). Then, step 8 to step 11 in Algorithm 1 will reduce to 6 flops. Hence, the total flops imposed for SM systems employing the conventional star-*M*QAM constellation [13] or any multiple-ring constellation adopting this specific orientation [23] is $\delta_{conventional\ star-MQAM} = (6N_R+13)N_T$. Note that this algorithm will achieve optimal-ML error performance.

4.2. Evaluation of Computational Complexity

In this subsection, we evaluate the computational complexity at the receiver, in terms of the total number of flops, as a function of constellation size M, number of receive antennas N_R and number of transmit antennas N_T. The computational complexity of the proposed detectors as well as the closest competing detectors are summarized in Table 2.

Table 2: Comparisons of Computational Complexity

Detectors	**Computational Complexity**	**Complexity grows with M?**
ML Detection [3]	$\delta_{\mathrm{ML}} = 6N_R N_T M$	Yes
DBD [6]	$\delta_{\mathrm{DBD}} = N_T(6N_R+4+2M) + p(4N_R+2)$	Yes
MMRC Detection [4]	$\delta_{\mathrm{MMRC}} = 6N_R N_T + 4N_T + 6M$	Yes
MS Detection [4]	$\delta_{\mathrm{MS}} = 6N_R N_T + 4N_T + 6\bar{N}M$	Yes
SVD [9]	$\delta_{\mathrm{SVD}} = (6N_R+4)N_T + 2N_R + 6N_R M$	Yes
PSOD	$\delta_{\mathrm{PSOD}} = 6N_R N_T + 4N_T + 17\bar{N}$	No
POD	$\delta_{\mathrm{POD}} = (6N_R+19)N_T$	No

From Figure 3(a), a 4×4 SM system is considered with the size of M changing according to the 2R-STAR-16QAM, 4R-STAR-64QAM and 8R-STAR-256QAM constellations. It can be seen that the complexity of the proposed detectors does not grow with M.

In Figure 3(b), we show the computational complexities by changing N_R when N_T and M are fixed at 4 and 16 (2R-

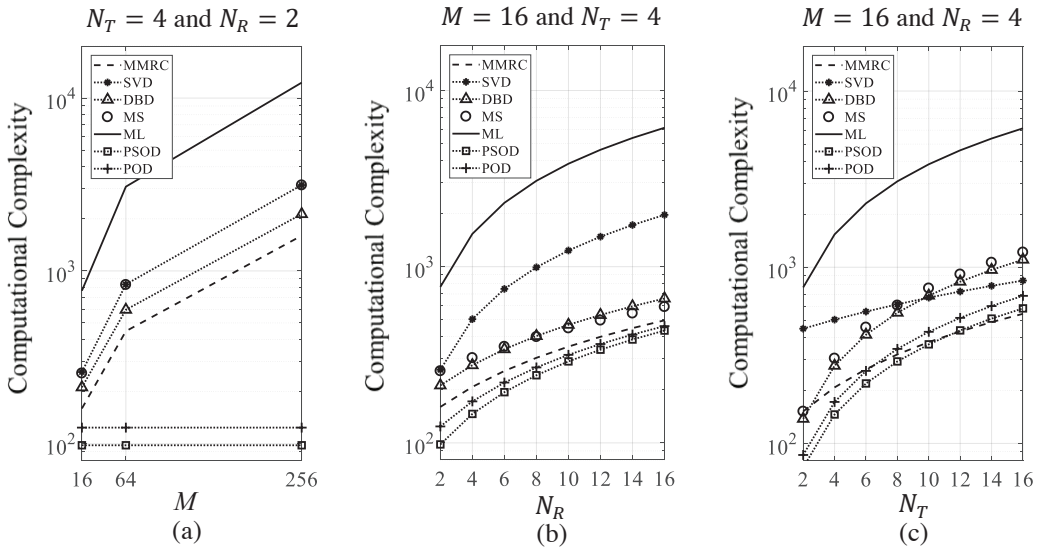

Figure 3: Comparisons of the computational complexity of the ABER performance for the proposed detectors and existing detectors as a function of (a) Constellation size M (b) Number of receive antennas N_R (c) Number of transmit antennas N_T. Note that $\bar{N} = \left(\frac{1}{2}\right) N_T$ for both the PSOD and MS detector. In addition, for DBD, the parameter $p = \left(\frac{1}{2}\right) N_T$.

STAR-16QAM), respectively. The results show that the proposed detectors offer much reduced complexities than the other notable detectors.

Finally, in Figure 3(c), we consider the computational complexity when $N_R = 4$ and $M = 16$ (2R-STAR-16QAM), while varying N_T. Though the computational complexity of the MMRC detector is lower than the proposed detectors when N_T is large, it has a non-negligible performance loss, which can be seen in Figure 5 - Figure 7.

In the next section, we present the Monte Carlo simulation results in terms of ABER performance for the proposed near-ML detectors in *N*R-STAR-*M*QAM-SM systems.

5. NUMERICAL ANALYSIS

The aim of this section is to evaluate and compare the ABER performance of the proposed detectors, which was presented in Section 3, to a few other low-complexity SM detectors, namely, MMRC detection [4], SVD [9], DBD [6], MS detection [4] and the benchmark ML-based detection [3]. As mentioned earlier, the proposed sub-optimal detector and proposed optimal detector are dubbed PSOD and POD, respectively, for ease of use. The simulation results are investigated over i.i.d. Rayleigh frequency-flat fading channels. Here the ABER is plotted against the average SNR at each receive antenna. As stated earlier, the spectral efficiency of SM is given as $\log_2(N_T M)$ bits per channel use (bpcu).

5.1. Evaluation and Comparison of the ABER Performance

The variance, which is normalized to one, is given as $\sigma^2 = E\left\{\left|\frac{\boldsymbol{s}_{APM}}{NF}\right|^2\right\} = 1$, where NF and $\boldsymbol{s}_{APM}$, represents the normalizing factor and symbol set of the employed APM constellation, respectively. Here, we denote the symbol set for the 2R-STAR-16QAM, 4R-STAR-64QAM and 8R-STAR-256QAM constellations as $\boldsymbol{s}_{2R\star16}$, $\boldsymbol{s}_{4R\star64}$ and $\boldsymbol{s}_{8R\star256}$, respectively.

In Figure 4, we compare the ABER of the detection algorithms presented in [12], namely PHD and PMML along with ML, PSOD and POD in 32-APSK-SM. Note that the ML detector is used for benchmarking purposes. The 32-APSK-SM system achieves a spectral efficiency of 7 bpcu and has radii $= (1, 2.5, 4)$ with $\sigma^2 = E\left\{\left|\frac{\boldsymbol{s}_{32-APSK}}{10.47}\right|^2\right\} = 1$, where $\boldsymbol{s}_{32-APSK}$ represents the symbol set of 32-APSK. It can be seen that the ABER performance of PHD and PMML closely matches the ABER performance of PSOD and POD, respectively.

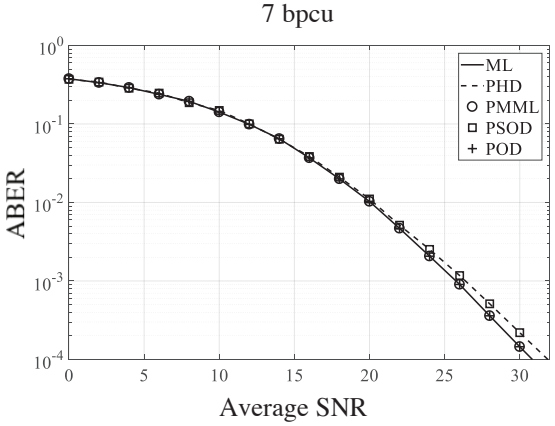

Figure 4: Comparison of ABER performance for 32-APSK-SM with $N_T = 4$ and $N_R = 2$ employing the following detectors: ML, PHD, PMML, PSOD and POD for a spectral efficiency of 7 bpcu.

The following analysis is performed in SM employing the 2R-STAR-16QAM, 4R-STAR-64QAM and 8R-STAR-

256QAM constellations with $N_T = 4$ and $N_R = 2$. In order to support the Monte Carlo simulation results, a closed-form union-bound theoretical ABER is provided for *N*R-STAR-*M*QAM [22].

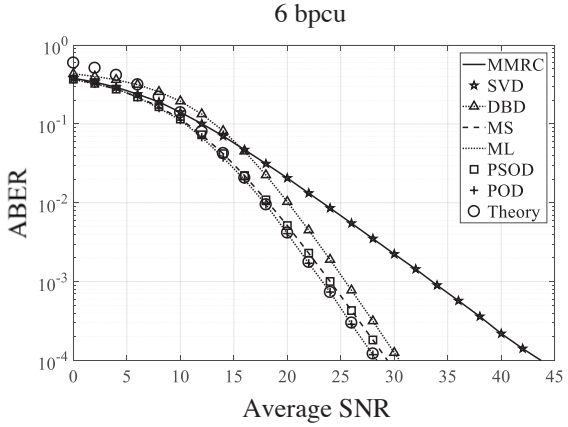

Figure 5: Comparison of ABER performance for 2R-STAR-16QAM-SM employing the following detectors: MMRC, SVD, DBD, MS, ML, PSOD and POD for a spectral efficiency of 6 bpcu.

In Figure 5, the 2R-STAR-16QAM-SM system has radii $= (1, 1.8)$ with $\sigma^2 = E\left\{\left|\frac{s_{2R\star16}}{2.12}\right|^2\right\} = 1$ and achieves a spectral efficiency of 6 bpcu. Note, the optimum radii for *N*R-STAR-*M*QAM-SM is efficiently calculated using the optimum ring radii algorithm in [22]. It can be seen that the POD matches very closely with the benchmark ML detector and that the theoretical expression, which was derived in [22], confirms this observation. Although, the PSOD has a slight deviation from the ML detector after 12 dB, it still has a superior error performance than the other detectors. At an ABER of 10^{-4}, the POD achieves an SNR gain of approximately 1 db compared to both the PSOD and MS detection. Also, when compared to DBD and both MMRC detection and SVD, the POD achieves an SNR gain of 2 dB and 15 dB, respectively.

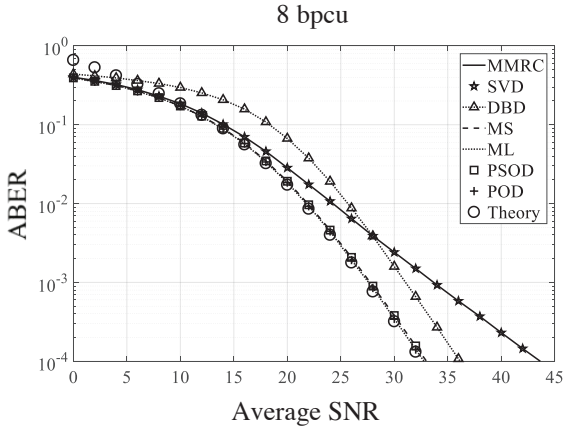

Figure 6: Comparison of ABER performance for 4R-STAR-64QAM-SM employing the following detectors: MMRC, SVD, DBD, MS, ML, PSOD and POD for a spectral efficiency of 8 bpcu.

In Figure 6, the spectral efficiency is increased to 8 bpcu by employing the 4R-STAR-64QAM constellation in SM. The optimal radii for this system is $(1, 1.5, 2.0, 2.5)$ with $\sigma^2 = E\left\{\left|\frac{s_{4R\star64}}{3.38}\right|^2\right\} = 1$. These simulation results, exhibit analogous ABER performances compared to Figure 5. For example, at an ABER of 10^{-4}, the proposed detectors achieve an SNR gain of approximately 3 dB compared to DBD and 11 dB compared to both the MMRC detection and SVD.

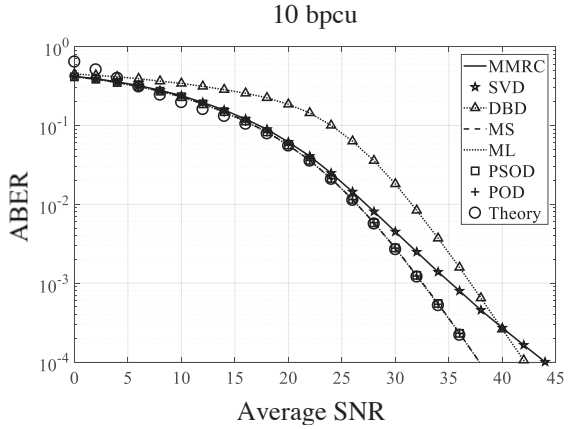

Figure 7: Comparison of ABER performance for 8R-STAR-256QAM-SM employing the following detectors, MMRC, SVD, DBD, MS, ML, PSOD and POD for a spectral efficiency of 10 bpcu.

In Figure 7, similar behaviour to Figure 5 and Figure 6 are demonstrated by the proposed detectors. The 8R-STAR-256QAM-SM system has an optimal radii of $(1, 1.3, 1.6, 1.9, 2.2, 2.5, 2.8, 3.1)$ with $\sigma^2 = E\left\{\left|\frac{s_{8R\star256}}{4.68}\right|^2\right\} = 1$. Here the MS detector, ML detector, PSOD and POD exhibit approximately the same error performance down to an ABER of 10^{-4}. At the same ABER, the proposed detectors achieve SNR gains of 4 dB and 6 dB compared to DBD and both the MMRC detector and SVD. Hence, these proposed detectors may prove to be a feasible alternative to the other notable detectors due to its superior ABER performance and lower computational complexity.

6. CONCLUSION

In this paper, we have proposed two low-complexity near-ML detection algorithms for SM systems suitable for employing any constellation from the star-*M*QAM family, more specifically the *N*R-STAR-*M*QAM constellation. We have provided a detailed computational complexity comparison of the proposed detectors and existing notable detectors. It has been shown that the computational complexity imposed by the proposed detectors are independent of both the size of the symbol set and the number of rings presented in the *N*R-STAR-*M*QAM constellation. This effectively means that the complexity is only dependent on the number of transmit antennas in the system. Hence, the proposed near-ML detectors are capable of offering near-ML error performance but at a

much reduced computational complexity. Furthermore, the ABER results have been supported by a closed-form union-bound theoretical solution.

REFERENCES

[1] R. Y. Meshleh, H. Haas, S. Sinanovic, C. W. Ahn and S. Yun, "Spatial modulation," *IEEE Transactions on Vehicular Technology,* vol. 57, no. 4, pp. 2228-2241, Jul. 2008.

[2] M. Di Renzo, H. Haas, and P. M. Grant, "Spatial modulation for multiple-antenna wireless systems: A survey," *IEEE Communications Magazine*, vol. 49, no. 11, pp. 182-191, Nov. 2011.

[3] J. Jeganathan, A. Ghrayeb, and L. Szczecinski, "Spatial modulation: Optimal detection and performance analysis," *IEEE Communications Letters*, vol. 12, no. 8, pp. 545-547, Aug. 2008.

[4] N. R. Naidoo, H. Xu, and T. A. Quazi, "Spatial modulation: optimal detector asymptotic performance and multiple-stage detection," *IET Communications*, vol. 5, no. 10, pp. 1368-1376, Aug. 2011.

[5] H. Xu, "Simple low-complexity detection schemes for *M*-ary quadrature amplitude modulation spatial modulation," *IET Communications*, vol. 6, no. 17, pp. 2840-2847, Nov. 2012.

[6] Q. Tang, Y. Xiao, P. Yang, Q. Yu, and S. Li, "A new low-complexity near-ML detection algorithm for spatial modulation," *IEEE Wireless Communications Letters*, vol. 2, no. 1, pp. 90-93, Feb. 2013.

[7] A. Younis, S. Sinanovic, M. Di Renzo, R. Meshleh, and H. Haas, "Generalised sphere decoding for spatial modulation," *IEEE Transactions on Communications*, vol. 61, no. 7, pp. 2805-2815, Jul. 2013.

[8] R. Rajashekar, K. V. S. Hari, and L. Hanzo, "Reduced-complexity ML detection and capacity-optimized training for spatial modulation systems," *IEEE Transactions on Communications*, vol. 62, no. 1, pp. 112-125, Jan. 2014.

[9] J. Wang, S. Jia, and J. Song, "Signal vector based detection scheme for spatial modulation," *IEEE Communications Letters*, vol. 16, no. 1, pp. 19-21, Jan. 2012.

[10] N. Pillay and H. Xu, "Comments on "Signal vector based detection scheme for spatial modulation"," *IEEE Communications Letters*, vol. 17, no. 1, pp. 2-3, Jan. 2013.

[11] H. Men and M. Jin, "A low-complexity ML detection algorithm for spatial modulation systems with *M*PSK constellation," *IEEE Communications Letters*, vol. 18, no. 8, pp. 1375-1378, Aug. 2014.

[12] L. Cong, Y. Huang, M. D. Renzo, J. Wang, and Y. Cheng, "Low-complexity ML detection for spatial modulation MIMO with APSK constellation," *IEEE Transactions on Vehicular Technology*, vol. 64, no. 9, pp. 4315-4321, May 2015.

[13] S. Dutta and A. Chandra, "Accurate SER expressions for *M*-ary dual ring star QAM in fading channels," *in Proceedings of the International Conference on Communications, Devices and Intelligent Systems (CODIS)*, pp. 1-4, Dec. 2012.

[14] R. De Gaudenzi, A. G. iFabregas, and A. Martinez, "Performance analysis of turbo-coded APSK modulation over nonlinear satellite channels," *IEEE Transactions on Wireless Communications*, vol. 5, no. 9, pp. 2396-2407, Sep. 2006.

[15] P. Yang, Y. Xiao, B. Zhang, S. Li, M. El-Hajjar and L. Hanzo, "Star-QAM signaling constellations for spatial modulation," *IEEE Transactions on Vehicular Technology*, vol. 63, no. 8, pp. 3741-3749, Oct. 2014.

[16] R. Muller, U. Wachsmann, and J. Huber, "Multilevel coding for peak power limited complex Gaussian channels," *in Proceedings of the IEEE International Symposium on Information Theory*, pp. 103, Jul. 1997.

[17] A. Younis, N. Serafimovski, R. Meshleh, and H. Haas, "Generalised spatial modulation," *in Proceedings of the Signals, Systems and Computers Conference,* pp. 1498-1502, Nov. 2010.

[18] J. Wang, S. Jia, and J. Song, "Generalised spatial modulation system with multiple active transmit antennas and low complexity detection scheme," *IEEE Transactions on Wireless Communications,* vol. 11, no. 4, pp. 1605-1615, Apr. 2012.

[19] Y. Xiao, Z. Yang, L. Dan, P. Yang, L. Yin, and W. Xiang, "Low-complexity signal detection for generalised spatial modulation," *IEEE Communications Letters,* vol. 18, no. 3, pp. 403-406, Mar. 2014.

[20] W. Liu, N. Wang, M. Jin, and H. Xu, "Denoising detection for the generalised spatial modulation system using sparse property," *IEEE Communications Letters,* vol. 18, no. 1, pp. 22-25, Jan. 2014.

[21] C.-T. Lin, W.-R.Wu, and C.-Y. Liu, "Low-complexity ML detectors for generalised spatial modulation systems," *IEEE Transactions on Communications,* vol. 63, no. 11, pp. 4214-4230, Nov. 2015.

[22] R. Pillay, H. Xu, and N. Pillay, "Antenna selection for *N*R-STAR-*M*QAM spatial modulation," *IET Communications*, vol. 11, no. 7, pp. 985-992, May 2017.

[23] L. Yu, T. Zhang, and C. Feng, "Symbol error rate comparisons of star *M*QAM schemes based on equal cubic metric," *in Proceedings of the 21st International Conference on Telecommunications (ICT)*, pp. 369-373, May 2014.

[24] M. Maleki, H. R. Bahrami and A. Alizadeh, "Constellation design for spatial modulation," *in*

Proceedings of the IEEE International Conference on Communications (ICC), pp. 2739-2743, Sep. 2015.